Detection and modeling of Road Traffic Events using Seismic Array

Pengchao He*, Haoran Meng, Zaiwang Liu, Yahao Zhao, Fuhua Zheng, and Mijia Chai, Die Yuan

Email: pengchao.he@mines.edu

Department of Earth and Space Sciences, Southern University of Science and Technology, Shenzhen 518055, China

Abstract

The ground motion induced by road traffic constitutes a significant component of seismic records in urban areas. Resolving road traffic events is essential for advancing our understanding of complex seismic waveforms. In this study, we introduce a series of algorithms designed for the detection of vehicular events and the extraction of key characteristics pertaining to the moving sources using seismic nodal array. Our research offers valuable insights into the dynamics of urban ground motion and holds potential for improving the imaging of subsurface structures.

Keywords: Vehicle traffic events detection, seismic seismometer, back projection method

Introduction

Seismometers have long been utilized to capture the vibrational signatures of natural earthquakes, and they are also capable of detecting signals stemming from human activities, including rail and road traffic events. Employing seismic records for the detection of vehicular events represents a pioneering application of seismology in the realm of traffic monitoring. This study aims to quantitatively discern the movement parameters of vehicular events through a series of experiments, comparing the efficacy of different detection algorithms. On November 1st, 2023, we conducted an experiment using 18 IMU-3C Smart-Solo nodes positioned along an urban roadside (see Figure 1). The nodes recorded continuously at a sampling rate of 500 Hz and captured hundreds of vehicular events. This research not only expands the horizons of seismological applications but also holds the potential for enhancing the precision of traffic monitoring systems.

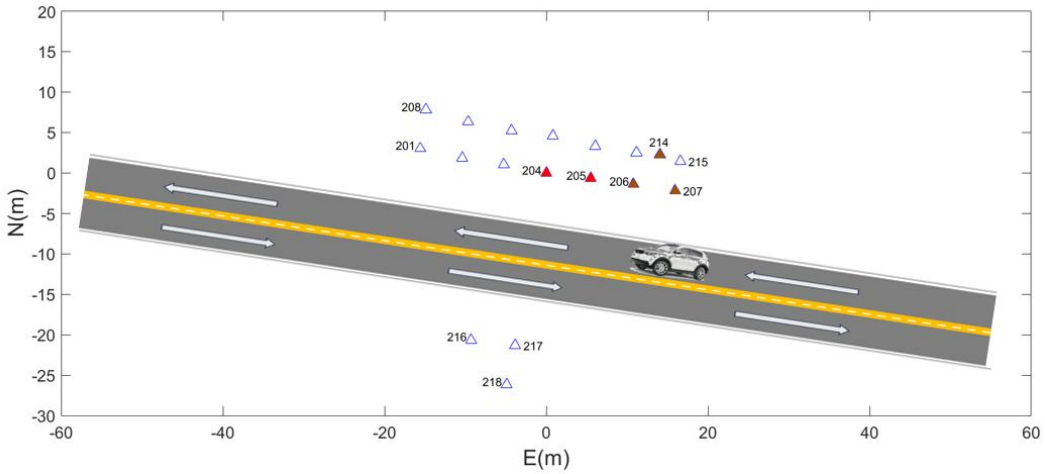

Figure 1. Experimental setup along an urban roadside. The blue triangles represent the locations of the Smart-Solo nodes deployed. The red and brown filled triangles represent the sites used as cases of the dual-station method and triple-station method respectively.

Methods

In this experiment, we employ four detection algorithms: the single-station method, the dual-station method, the triple-station method, and the array-based method.

The single-station method is designed to detect vehicle events and generate a detection catalog using data from a single seismometer (Figure 2a). Its principle lies in the interaction between passing vehicles and the pavement, which generates ground vibrations recorded by the seismometer. When the amplitude of these recorded vibrations exceeds a predetermined threshold, it indicates the presence of a vehicle within the monitoring area. Subsequently, when the seismic wave amplitude returns below the threshold after a few seconds, it signifies the departure of the vehicle from the monitoring area (Meng et al., 2020). Moreover, the size of the vehicle can be estimated based on the amplitude and duration of the vibrations it induces. Generally, heavier vehicles produce vibrations with greater amplitude and longer duration, while smaller vehicles exhibit lower amplitude and shorter duration. Therefore, multiplying the amplitude of the vibrations by the duration of the vehicle event can serve as a quantitative measure of the vehicle's size.

The dual-station method uses two seismometers placed a certain distance apart (e.g., 5 meters) and aligned parallel to the road. By analyzing differences in the arrival times of vehicle-induced vibrations recorded by each seismometer, this method can determine both the speed and direction of the vehicle. The vehicle's speed is inferred from the slope of the arrival time difference curve, while its direction is determined by the curve's orientation. This method is illustrated in Figure 2b, where the red curve represents a vehicle traveling at 30 m/s, the black curve at 20 m/s, and the blue curve at 10 m/s. Variations in travel times are clearly visible for different speeds. Additionally, changes in the vehicle's direction can alter the sequence in which seismic signals reach each seismometer, thereby affecting the direction of the arrival time difference.

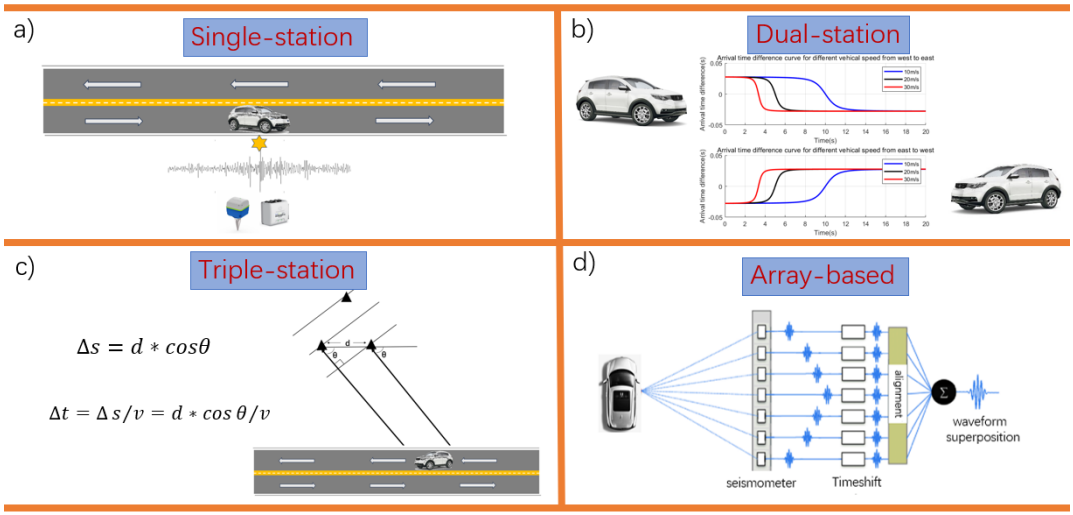

Figure 2. Diagram depicting the operational principles of four algorithms: (a) the single-station method, (b) the dual-station method, (c) the triple-station method, and (d) the array-based method.

The triple-station method uses three equidistant seismometers to determine a vehicle's azimuth and changes in azimuth to infer its direction and speed. This method assumes that the surface waves generated by the vehicle's movement are plane waves. The distance between the stations is represented as d, and the angle between the line connecting the vehicle and the array and the direction of the road is denoted as θ. As depicted in Figure 3, the path difference of the wavefront arriving at the station is given by $\Delta s = d\cos\theta$, resulting in an arrival time difference of $\Delta t = \Delta s / v = d\cos\theta / v$, where v represents the seismic wave velocity. By establishing a relationship between the arrival time differences among the three seismometers and the vehicle's azimuth, this method can determine the vehicle's specific location and, consequently, its speed, given a known road geometry.

The array-based method utilizes a seismic array comprising multiple seismometers to track a vehicle's trajectory using the waveform beamforming method. When a vehicle passes a point on the ground, it generates a vibration signal received by all seismometers in the array. However, due to varying distances between the vehicle and each seismometer, the arrival times of the signals differ. Assuming the vehicle travels to a specific position at a certain time, the arrival time differences of the waveform signals at each seismometer can be calculated. By shifting and superimposing the waveforms based on these arrival time differences, the method aligns waveform phases for each seismometer. If the assumed vehicle position matches the actual position, the aligned waveforms will result in a maximum amplitude (as shown in Figure 2d). Conversely, a large deviation in the assumed position will lead to misaligned phases and reduced waveform amplitudes upon superposition. Therefore, by conducting a grid search along the road, the method can determine the vehicle's position at each moment, enabling the reconstruction of its trajectory.

Results

Based on the single-station method, segments of the time-domain waveform exceeding a predefined threshold are identified and marked as a red band, as depicted in Figure 3. This red band represents the time window during which the vehicle-induced waveform is present within the monitoring area. The start and end of this band signify the vehicle's entry into and exit from the monitored zone, respectively. Table 1 provides details on each vehicle's entry and exit times, along with the event duration and peak time, which corresponds to when the vehicle-induced vibration signal reaches its maximum. Additionally, Table 1 includes vehicle type information, distinguishing between heavy and small vehicles.

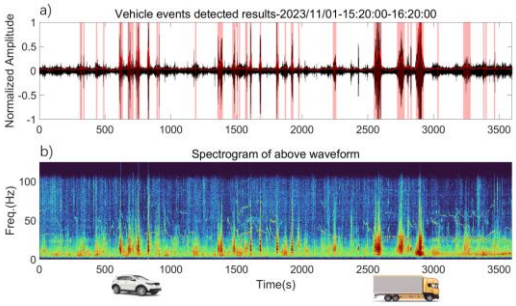

Figure 3. (a) Vertical waveform recorded by node #204 from 15:20:00 to 16:20:00 on November 1st, 2023, local time at GMT+8. Detected events are indicated by the light red strips. (b) Corresponding spectrogram.

Vehicle No.	Starting clock	Peak clock	End clock	Duration(s)	Vehicle size	Vehicle type
1	15:25:09	15:25:14	15:25:19	10	7.59	Small
2	15:25:30	15:25:35	15:25:40	10	7.46	Small
3	15:27:14	15:27:19	15:27:24	10	8.02	Small
4	15:28:05	15:28:10	15:28:15	10	7.26	Small
5	15:30:05	15:30:16	15:30:36	31	113.25	Small
6	15:31:12	15:31:25	15:31:57	45	171.06	Small
7	15:32:13	15:32:34	15:32:45	32	177.25	Small
8	15:33:46	15:33:51	15:33:56	10	51.02	Small
9	15:34:52	15:34:57	15:35:02	10	7.19	Small
10	15:39:50	15:39:55	15:40:00	10	8.14	Small
11	15:42:35	15:43:08	15:43:17	42	117.47	Small
12	15:44:30	15:44:44	15:44:53	23	49.01	Small
13	15:45:04	15:45:09	15:45:14	10	7.12	Small
14	15:45:18	15:45:23	15:45:28	10	8.20	Small
15	15:45:58	15:46:03	15:46:08	10	8.31	Small
16	15:46:15	15:46:20	15:46:25	10	7.96	Small
17	15:46:45	15:46:50	15:46:55	10	29.85	Small
18	15:47:58	15:48:03	15:48:08	10	29.05	Small
19	15:50:01	15:50:10	15:50:21	20	55.80	Small
20	15:51:08	15:51:13	15:51:18	10	9.46	Small
21	15:52:01	15:52:06	15:52:11	10	27.11	Small
22	15:52:51	15:52:56	15:53:01	10	10.00	Small
23	15:57:15	15:57:31	15:57:40	25	36.28	Small
24	16:02:27	16:03:01	16:03:24	57	287.94	Large
25	16:05:24	16:05:55	16:06:21	57	195.95	Large
26	16:06:43	16:06:48	16:06:53	10	12.74	Small
27	16:07:06	16:07:11	16:07:16	10	7.90	Small
28	16:07:46	16:08:16	16:08:47	61	706.22	Large
29	16:13:47	16:14:26	16:14:43	56	68.96	Small
30	16:15:51	16:15:56	16:16:01	10	7.51	Small
31	16:16:19	16:16:24	16:16:29	10	7.14	Small
32	16:16:36	16:16:41	16:16:46	10	7.03	Small
33	16:17:41	16:17:46	16:17:51	10	8.63	Small

Table 1. The detection catalog for the single-station method pertaining to the waveform displayed in Figure 3

As an illustration of the dual-station method, the seismic array records from station #204 and #205 in Figure 4 are cross-correlated to produce the arrival time difference curve for the waveform signal within a 15-second time window centered around 13:20:09. Fitting this curve yields the determination that the vehicle is moving from east to west at a speed of 36 km/h. Similarly, by cross-

correlating the waveform within a 10-second time window around 15:33:50, we determine that the vehicle is moving from west to east at a speed of 42 km/h.

As an example of the dual-station method, the vertical waveforms recorded by nodes #204 and #205 in Figure 4 are cross-correlated, resulting in the arrival time difference curve for the waveform signal within a 15-second time window centered around 13:20:09. By fitting this curve, the vehicle's direction and speed are determined to be moving from east to west at a speed of 36 km/h. Similarly, analyzing the waveform within a 10-second time window around 15:33:50 yields the conclusion that the vehicle is moving from west to east at a speed of 42 km/h. The effective range is estimated by the vehicle speed and the event duration. Assuming the vehicle travels at a constant speed in a straight line at the detected speed of 36 km/h, i.e., 10 m/s, the effective detection distance of the dual-station method is approximately 10 m/s*30 s=300 m.

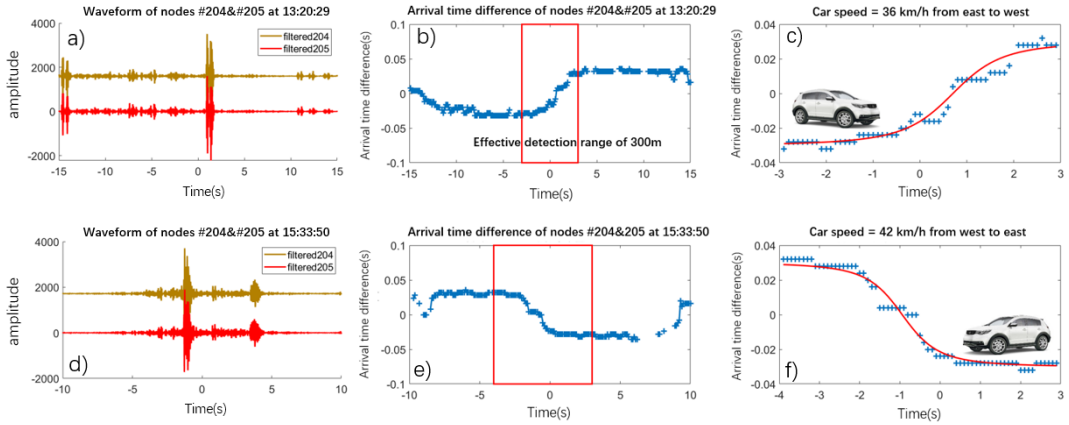

Figure 4. (a)(d) The vertical waveform recorded by nodes #204 and #205, November, 1st, 2023, GMT+8. (b) (e)The observed differential arrival time. (c)(f) The deduced direction and speed of the vehicle movement.

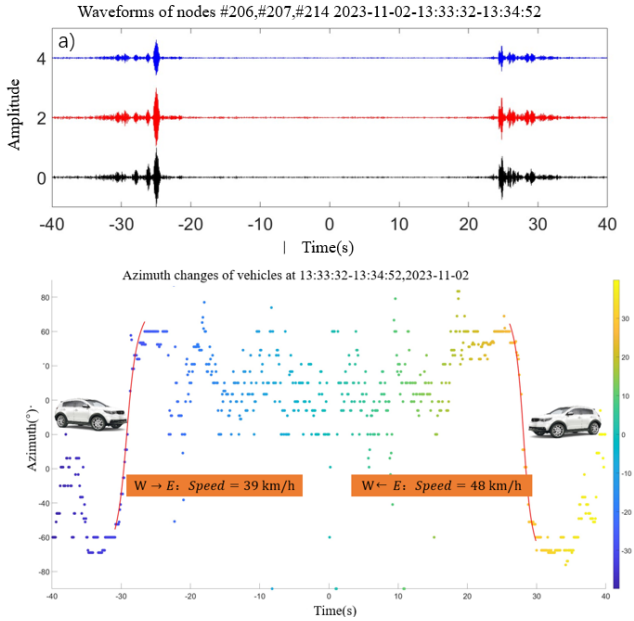

Figure 5. (a) Vertical waveforms recorded by nodes #206, #207, and #214 from 13:33:32 to 13:34:52, November, 2nd, 2023, GMT+8.. (b) The wave propagation angle change with time of two vehicular events.

Figure 5 displays the distribution and waveform records of three nodes arranged in an equilateral triangle configuration with a 5 m interstation distance. Cross-correlation of the waveforms provides the time differences necessary to determine changes in the azimuthal angles of the stations, as

depicted in Figure 5. When a vehicle enters the monitored region, the azimuthal angle of the energy source shows a significant monotonic increase or decrease. Notably, a transition from a negative to a rapidly increasing positive azimuthal angle indicates a vehicle moving from west to east, while a shift from a positive to a rapidly decreasing negative azimuthal angle signifies a vehicle moving from east to west. Conversely, when the azimuthal angle lacks a distinct pattern, it suggests background noise without vehicular activity. Additionally, vehicle speeds can be inferred by monitoring the change rate of the azimuthal angle over time, with steeper slopes corresponding to faster vehicles. This enables quantitative calculations, such as determining that a vehicle traveled from west to east at 39 km/h around 13:33:39 across the triangle array and from east to west at 48 km/h around 13:34:40, passing over the triangle array again.

Utilizing waveform beamforming analysis, Figure 6 illustrates the operational trajectory of a vehicle. This analysis effectively captures signals from rapidly moving vehicles and detects signals from pedestrian movements. Moreover, it accurately determines the speed of the signal's source based on variations in signal slope. Through waveform beamforming analysis, vehicle motion paths can be discerned, enabling effective monitoring regardless of whether the signal's source moves parallel or perpendicular to the road. The red box in Figure 6 indicates the type and speed of the source, encompassing signals from pedestrians, electric vehicles, cars, and more.

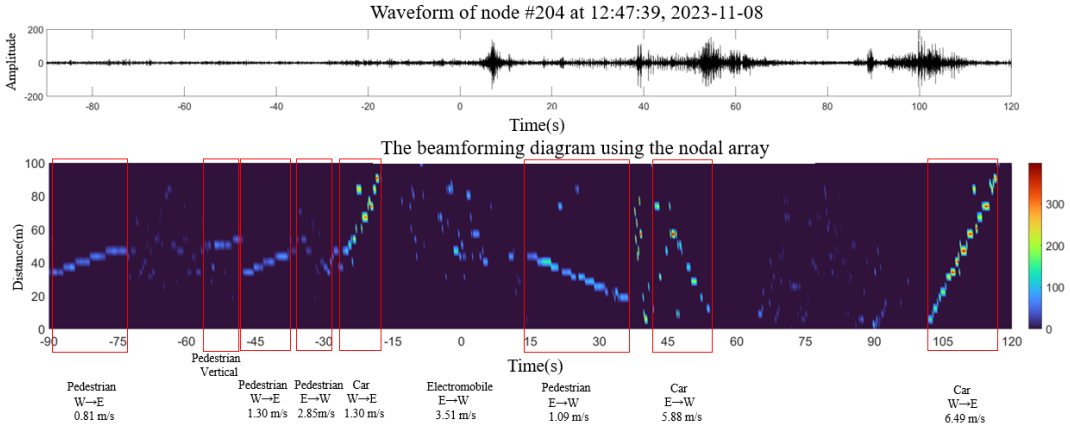

Figure 6. (a) Vertical waveforms recorded by node #204 at 12:47:39, November, 8th, 2023, GMT+8. (b) The beamforming diagram using the nodal array.

Conclusions

In this study, we introduce four algorithms to detect vehicular events and determine vehicle motion parameters from seismograph waveform data. The single-station method effectively detects vehicle entry and exit times and discriminates between vehicle types, but it cannot determine vehicle direction or speed. The dual-station method can determine vehicle direction and speed but requires stations to be parallel to the road, limiting its effectiveness for vehicles moving perpendicular to the station layout. The triple-station method can determine vehicle direction and speed without specific station layout requirements but assumes plane-wave propagation, introducing systematic errors in estimating vehicle speed. The array method can determine vehicle position and trajectory but requires more stations and computational effort, with reduced resolution in areas with substantial lateral heterogeneity due to the application of average wave velocity in beamforming.

References

Meng, H., Ben-Zion, Y., & Johnson, C.W. (2021). Analysis of Seismic Signals Generated by Vehicle Traffic with Application to Derivation of Subsurface Q-Values. Seismological Research Letters.